Journal of Petroleum Exploration and Production Technology (2023) 13:1085–1097
https://doi.org/10.1007/s13202-022-01584-0

ORIGINAL PAPER - PRODUCTION GEOPHYSICS

A new method of evaluating well-controlled reserves of tight gas sandstone reservoirs

Xiangdong Guo[1] · Min Lv[1] · Hongjun Cui[1] · Kaiyu Lei[1] · Yanyun Lei[1] · Yushuang Zhu[2]

Received: 27 August 2021 / Accepted: 4 November 2022 / Published online: 24 November 2022

Abstract

Based on static geology and dynamic production of typical wells in Yan'an gas field, a convenient method of the wells controlled reserves was established combining with material balance method (MB). The method was applied to 88 wells in Yan'an tight gas field. The results show that: ①Controlled by pore structure, wells are divided into three types based on the morphology of the capillary pressure curve and the analysis of the parameter characteristics, and their productivity is evaluated, respectively. ②The flow material balance method (FMB) ignores the change of natural gas compressibility, viscosity and Z in the calculation. After the theoretical calculation of 30 gas samples, the slope of the curve of the relationship between bottom hole pressure and cumulative production and the slope of the curve of the relationship between average formation pressure and cumulative production are not equal. ③Compared with the results of the MB, the result of the FMB is smaller, and the maximum error is 34.66%. The consequence of the modified FMB is more accurate, and the average error is 2.45%, which has good applicability. The established method is simple, only requiring production data with high precision, providing a new method to evaluate well-controlled reserves of tight gas sandstone. This method with significant application value can also offer reference values for other evaluating methods of well-controlled reserves.

Keywords Tight gas reservoir · Well-controlled reserves · Modified flowing material Balance · Yan'an gas field · Ordos Basin

Abbreviations

B_g	Volume coefficient of natural gas;
C_g	Natural gas compressibility;
$\overline{C}_g$	Compressibility of natural gas under average formation pressure, MPa^{-1};
C_{gwf}	Compressibility of natural gas under bottom hole pressure, MPa^{-1};
ETM	Elastic two-phase method;
FMB	Flow material balance method;
G_p	Cumulative gas production, 10^4m^3;
MB	Material balance method;
Modified FMB	Modified flow material balance method;
OFR	Open flow rate, $10^4m^3/d$;
P_{wf}	Bottom hole flow pressure, *MPa*;
P_{wfi}	Original bottom hole flow pressure, *MPa*;
$\overline{P}$	Average formation pressure, *MPa*;
$\overline{P}_{pss}$	Average formation pressure at the initial stage of pseudo steady state, *MPa*;
$P_{wf\text{-}pss}$	Bottom hole flow pressure at the initial stage of pseudo steady state, *MPa*;
P_i	Original formation pressure, *MPa*;
$\overline{u_g}$	Viscosity of natural gas under average formation pressure, *mPa·s*;
μ_{gwf}	Viscosity of natural gas under bottom hole flow pressure, *mPa·s*;
$\overline{Z}$	Z of natural gas under average formation pressure;
Z_{wf}	Z of natural gas under bottom hole flow pressure

✉ Yushuang Zhu
petroleum_gas@163.com

[1] No. 1 Gas Production Plant, Yanchang Oilfield Oil and Gas Exploration Company, Yan'an 716000, China

[2] State Key Laboratory of Continental Dynamics, Department of Geology, Northwest University, Xi'an 710069, China

Introduction

Located in the southeastern Ordos Basin, Yan'an gas field is the largest low-permeability tight sandstone field in China, producing more than $200 \times 10^8 m^3$ for three years from 2019 to 2022, and is also the largest natural gas field in terms of production in China (Clarkson 2013; Ning et al. 2009). The main gas producing layer of Yan'an gas field is He 8 member, with porosity ranging from 2.0 to 12.0% and permeability mainly in the range of 0.1 to 10.0 mD. It is a typical "low pressure, low porosity, low permeability and strong heterogeneity gas field" (Zou et al. 2012). The development of conventional straight wells faces difficulties such as low production, difficulty in stabilizing production and rapid pressure drop (Han et al. 2019). Therefore, it is necessary to analyze the production performance and its controlled reserves.

At present, the main methods for calculating dynamic reserves include MB (material balance method), the production decline method, production accumulation method, elastic two-phase method and so on, which are suitable for conventional reservoirs (Schmoker 2002; Wang et al. 2013; Zhang et al. 2008). Among them, the establishment of the material balance method is relatively easy with less data (Lyu et al. 2020; Muther et al. 2022a; Shults 2020). While there are no data such as bottom hole pressure, the MB cannot calculate the dynamic reserves of gas wells (Li et al. 2015; Zhenhua and Xinwei 2013). The FMB (flowing material balance method) does not take into account the effect of pressure on the viscosity and compressibility of gas, leading to an error in the result.

In order to solve the above problems, a modified FMB method is proposed in this study, in which the influence of pressure on the viscosity and compressibility of gas is considered. Taking the tight reservoir in Yanchang Oilfield in Ordos Basin as an example, the FMB and modified FMB are compared and analyzed.

Geological background

Ordos Basin is a large sedimentary basin with multi-cycle evolution and multi-sedimentary types. At present, the structure is a large syncline with slow width in the east and steep and narrow in the west, and the dip angle is generally less than 1° (Feng et al. 2016). Fault folds in the margin of the basin are well developed and the internal structure is relatively simple. There is no secondary structure in the basin, and the tertiary structure is dominated by nose uplift (Guo et al. 2018). According to the current structural shape, basement properties and structural characteristics of the basin, it can be divided into six units: Yimeng uplift, Weibei uplift, western Shanxi flexure fold belt, Yishan slope, Tianhuan depression and western margin thrust structural belt.

Yan'an gas field is located in the southeast of Yishan slope in Ordos Basin (Fig. 1) (Hu et al. 2008). The comprehensive geological study shows that the Upper Paleozoic in the area has many favorable conditions, such as extensive hydrocarbon generation, development of reservoir rock multi-layer system, wide distribution of regional caprock, which are beneficial to the formation and enrichment of large lithologic gas reservoirs (Hu et al. 2010; Muther et al. 2022b; Sun et al. 2020).

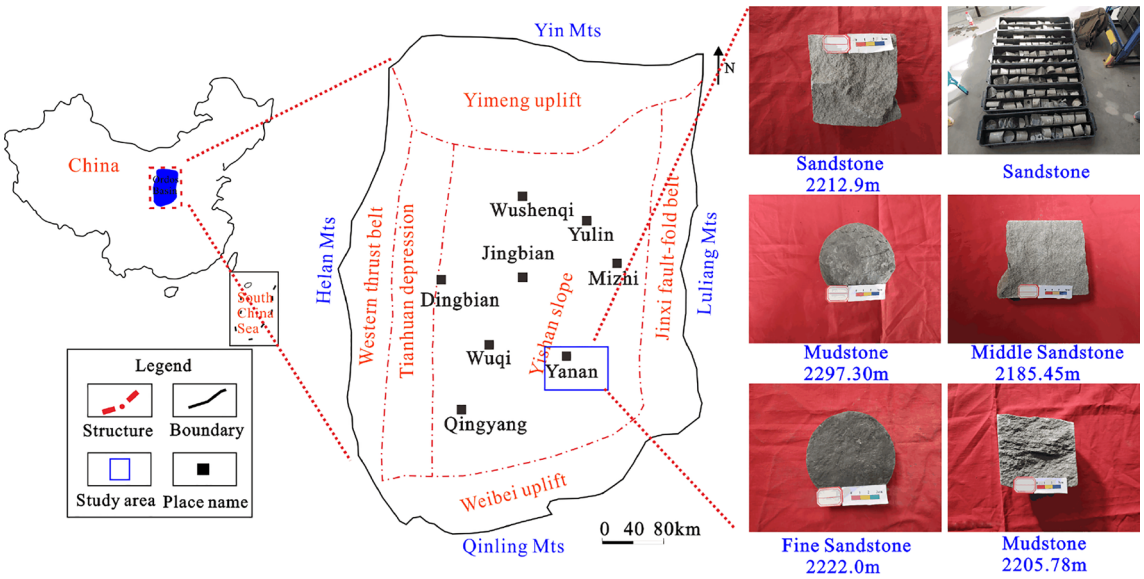

Fig. 1 Location map of Yan'an gas field in Ordos Basin

The sandstones are mainly gray-white, gray-green and dark gray, and the mudstones are mainly black and gray-black, containing a large number of plant fossils. The sedimentary in the study area is delta frontal sedimentation, and the microphases are mainly underwater distributary channel, interdistributary area and bank (Fig. 2). Controlled by the sedimentary, the sand body is north–south trending. The thickness is mainly distributed in 8–12 m, and the average thickness is 8.4 m.

Rock types are mainly quartz sandstone, followed by lithic quartz sandstone and lithic sandstone (Fig. 3). The fillings are dominated by silica, kaolinite, illite and iron calcite, and contain small amounts of iron chlorite, iron dolomite and hard gypsum. Observed by thin section, the storage space is mainly dominated by residual primary intergranular pores, dissolved intergranular pores, a small amount of intragranular dissolved pores, kaolinite intergranular pores and dissolved microfractures (Fig. 4, Fig. 5).

The pore structure can be divided into three types based on the morphology of the capillary pressure curve and

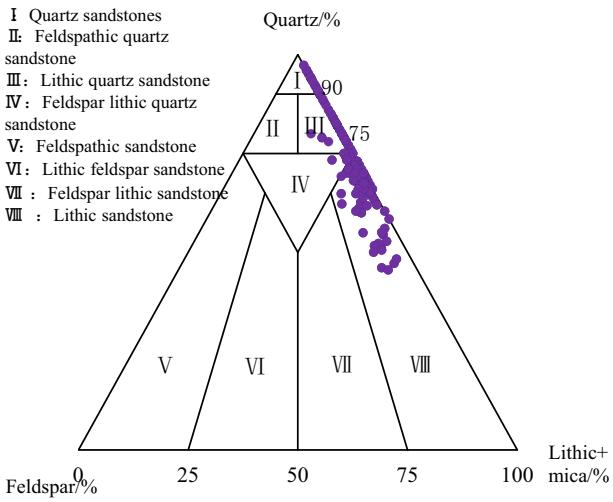

Fig. 3 Petrologic characteristics of reservoirs

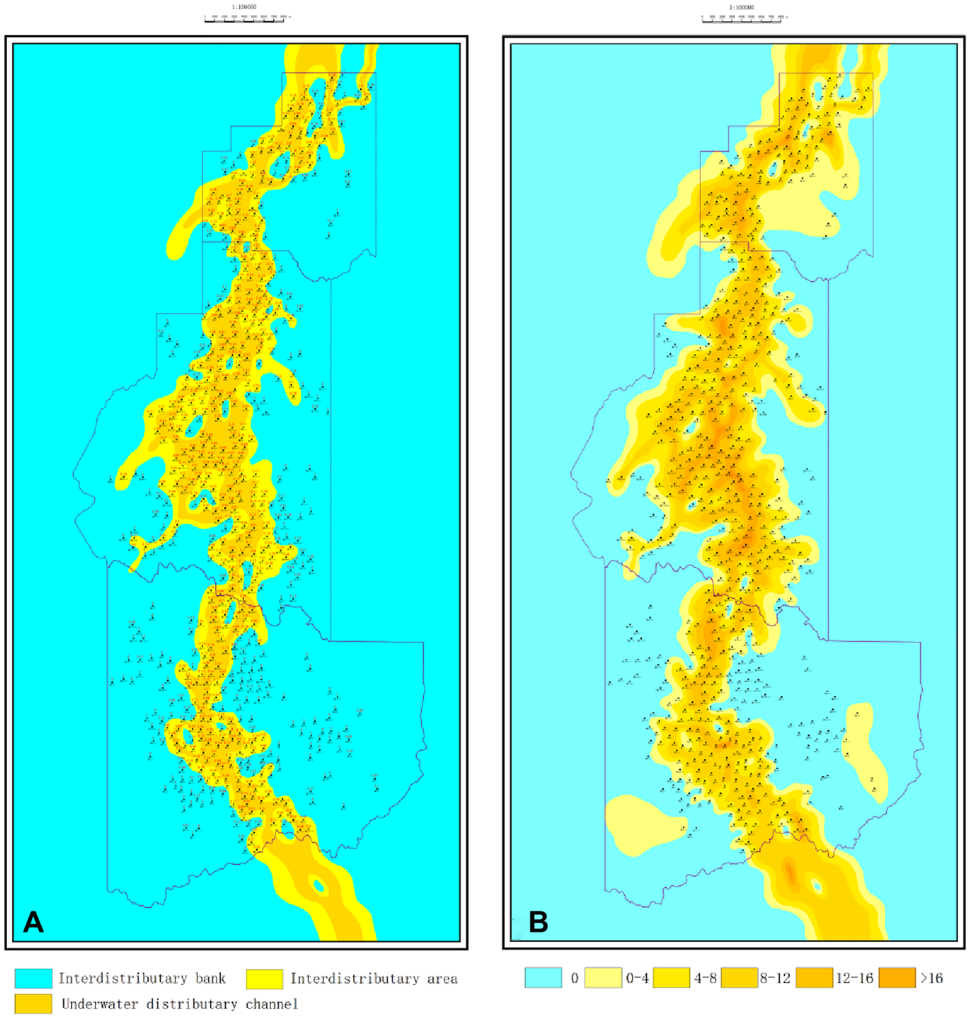

Fig. 2 Sedimentary facies and sand thickness of area (**A**: sedimentary facies; **B**: sand thickness)

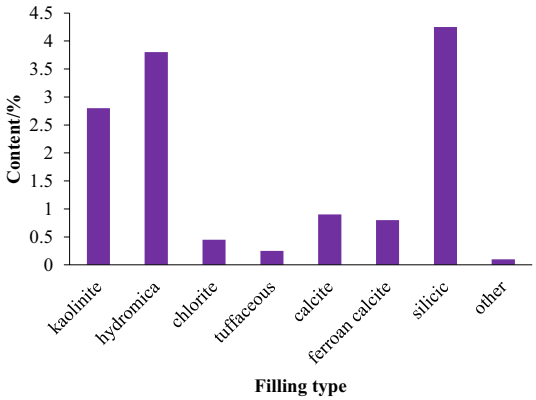

Fig. 4 Types of clay minerals

the analysis of the characteristics of the samples (Table.1, Fig. 6).

(1) Type-I

The curve is platform-shaped and slightly concave to the left. The discharge pressure is very low, mainly distributed in the range of 0.03 to 0.1 MPa, with an average pressure of 0.224 MPa. The average of pore throat radius is large, mainly distributed in the range of 1.41 to 4.12 μm, with an average radius of 3.35 μm; the throat distribution is coarse skewness, and the sorting is medium.

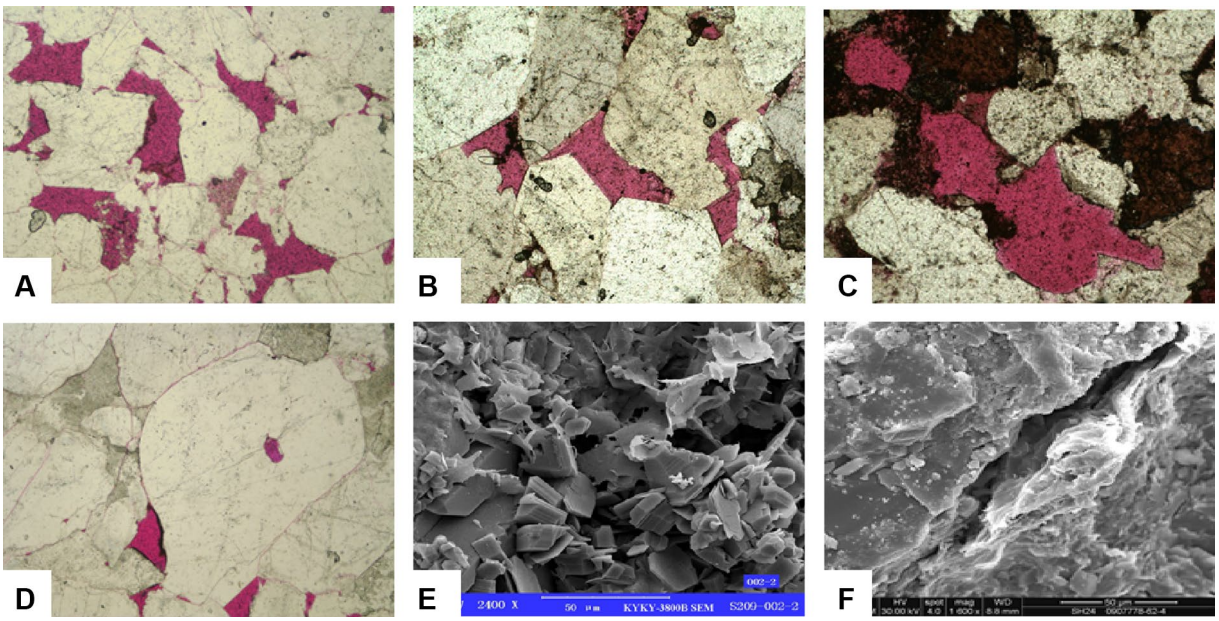

Fig. 5 Microscopic characteristics of the sandstone reservoirs. (**A**: residual intergranular pore, 2431.23 m; **B**: residual intergranular pore, 2727.07 m; **C**: intergranular dissolved pores, 2631.23 m; **D**: dissolved pores in grains, 2599.45 m; E: intercrystalline pore of kaolinite, 2629.63 m; F: microfracture, 2443.45 m)

Table 1 Classification of pore parameter

Parameter	Pore size			Pore characteristic				Pore connectivity	
Type	Displacement pressure /mD	Laryngeal coefficient	Radius /μm	Sorting coefficient	Relative sorting coefficient	Kurtosis	Skewness coefficient	Hg max/%	Mercury withdrawal efficiency /%
I	0.03–0.1	5.92–7.53	1.41–4.12	2.37–2.79	0.31–0.48	3.26–5.19	1.65–2.05	67.68–77.06	14.21–20.50
	0. 224	5.32	3.35	2.53	0.40	4.28	1.87	72.89	17.77
II	0.2–1.5	7.10–10.19	0.17–1.09	1.44–2.46	0.14–0.34	2.67–6.5	1.50–2.25	73.60–91.64	20.01–25.11
	0.52	8.39	0.69	2.14	0.27	4.12	1.82	80.40	22.97
III	0.4–1.5	8.70–10.71	0.14–0.44	2.41–3.40	0.24–0.35	2.17–3.59	1.43–1.8	73.05–83.65	38.00–45.23
	0.83	9.58	0.29	2.74	0.29	2.96	1.63	79.13	42.56

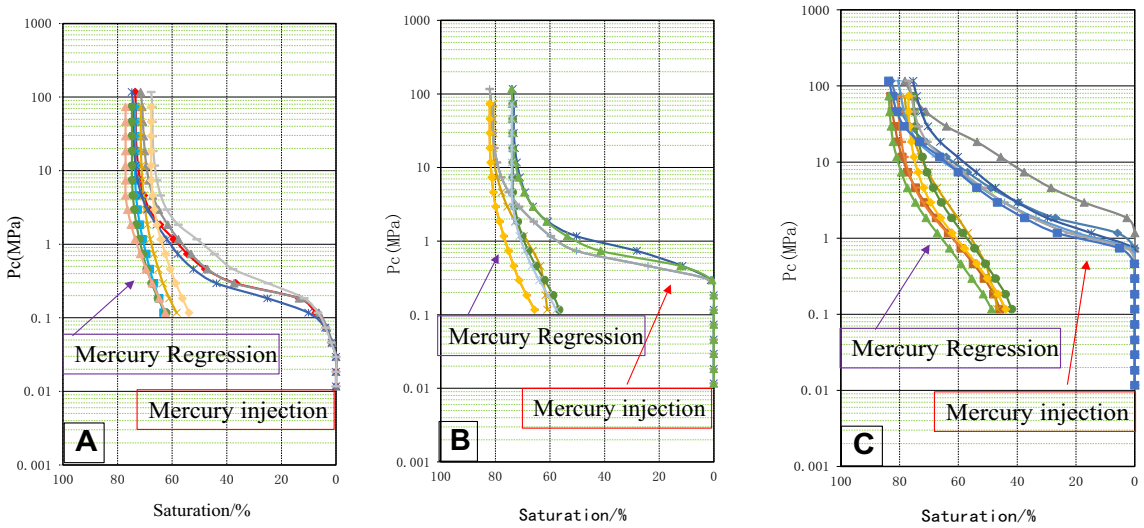

Fig.6 Classification of pore structure (**A**: Type-I; **B**: Type-II; **C**: Type-III)

(2) Type-II

The curve is gently sloping and also slightly concave to the left, with higher discharge pressure and median pressure than Type-I. The discharge pressure is mainly distributed in the range of 0.2 to 1.5 MPa, with an average of 0.52 MPa. The average radius of the pore throat is smaller than Type-I, mainly distributed in the range of 0.17 to 1.09 μm, with an average of 0.69 μm.

(3) Type-III

The discharge pressure of these reservoirs is medium, distributed in the range of 0.4 to 1.5 MPa. The capillary pressure curve is steeply sloping and the platform is not obvious. The pore throat radius is 0.14–0.44 μm and the sorting is poor.

Method

Due to the different conditions of methods, the results vary widely. According to the research on the geology of Yan'an gas field, the applicable methods for dynamic reserves in low-permeability tight sandstone reservoirs are the MB (material balance method) and the ETM (elastic two-phase method) (He et al. 2021; Luo et al. 2019; Zou et al. 2012).

Dynamic reserves calculation method

Material balance method

The MB uses a "pressure drop diagram" consisting of apparent formation pressure (P/Z) and cumulative production (G_p) to determine the dynamic reserves. However, it is not applicable to water-driven reservoirs and abnormally high pressure reservoirs (Andersen and Hyman 2001; Ruilan et al. 2010; Wei et al. 2016).

From the perspective of seepage mechanics, for closed reservoirs, the pressure wave is transmitted to the boundary of the formation after a certain period of relatively stable production, and the seepage enters the quasi-steady stage (Fig. 7). Mattar et al. proposed that formation pressure can be replaced by wellhead casing pressure and bottom hole pressure in MB (Fig. 8) (Mattar et al. 2006).

The elastic two-phase method

For a gas reservoir with a finite confinement of constant productivity, the pressure drop curve can be divided into three parts: unstable seepage early stage, unstable seepage late stage and pseudo steady (Fig. 9). At pseudo steady, the flow pressure at the bottom is linear with time (Fig. 10),

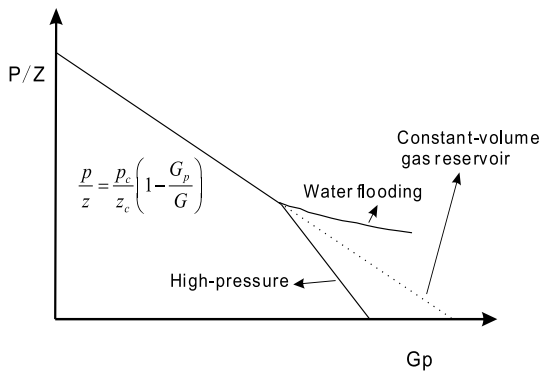

Fig. 7 Pressure depletion curve of reservoir

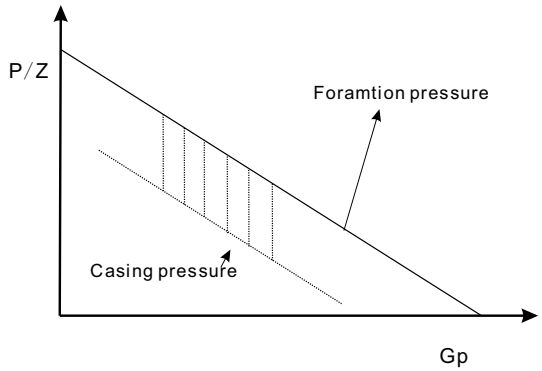

Fig. 8 Casing pressure depletion curve

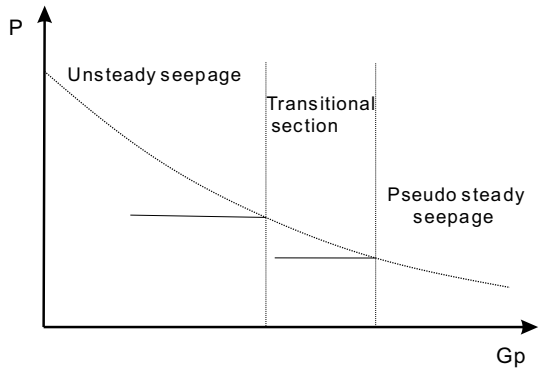

Fig. 9 Elastic two-phase theoretical curve

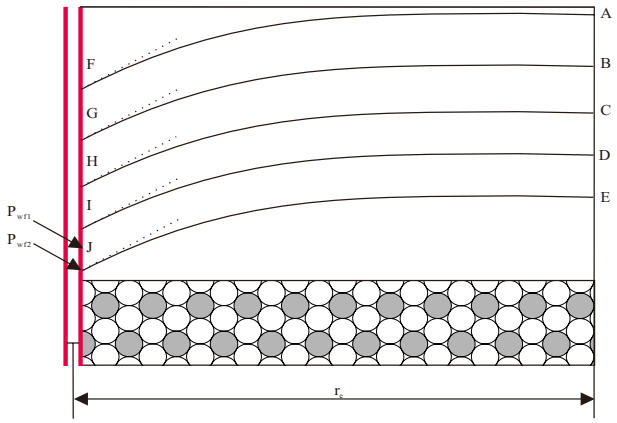

Fig. 10 Pressure profile of the well

which is used to determine the reserves (Kanianska et al. 2011; Long et al. 2011).

The ETM for evaluating control reserves requires the well to reach the pseudo steady stage (Han et al. 2019). If the production is too large, a "false steady state" is likely to occur, and the slope of the linear is larger than the true value, resulting in a smaller calculation. In addition, for tight reservoirs with low permeability, the pressure wave propagation is slow and it takes a long time, which results in high testing cost.

FMB method

Principle

When there are no data such as bottom hole pressure, the MB cannot calculate the dynamic reserves (Hirst et al. 2001; Nie et al. 2018; Ning et al. 2009). In order to solve this problem, Mattar put forward the FMB, which is analyzed from the point of view of percolation mechanics (Mattar et al. 2006). It is considered that the viscosity and compressibility of natural gas remain unchanged (Ning et al. 2009). However, when the formation pressure of the reservoir is low, the assumption is not valid.

In order to solve the problems, a modified FMB is proposed in this study, in which the influence of pressure on the viscosity and compressibility is considered. Taking the tight reservoir of Yan'an gas field in Ordos Basin as an example, the FMB and modified FMB are compared and analyzed.

Property of natural gas

(1) Viscosity

Through 30 gas samples (Tables.2, 3, 4) under the temperature of 352 K and pressure of 30 MPa, the viscosity of natural gas increases with the temperature under the condition of low pressure, and the viscosity increases with pressure (Fig. 11).

(2) Z coefficient

The Z at different temperatures and pressure can be gotten, as shown in Fig. 11. It decreases at first ($P < 15$ MPa) and then increases ($P > 15$ MPa).

(3) Compressibility

The relationship of P–C_g at different temperatures can be obtained (Fig. 11): the compressibility decreases with temperature and pressure.

(4) Volume coefficient

The volume coefficient decreases with pressure and increases with temperature (Fig. 11).

Modified FMB

In the FMB, it is assumed that the pressure has no effect on the viscosity and compressibility (Clarkson 2013; Li et al. 2015):

$$\partial\left(\overline{u_g}\,\overline{C_g}\right) = \partial\left(u_{gwf}C_{gwf}\right) \tag{1}$$

Table 2 Composition of 30 groups of natural gas samples-a

Sample	1	2	3	4	5	6	7	8	9	10
CH_4/%	96.41	96.485	94.061	95.89	96.891	97.3	97.099	97.534	97.087	97.251
C_2H_6/%	0.343	0.442	0.284	0.509	0.514	0.685	0.627	0.657	0.638	0.610
C_3H_8/%	0.019	0.025	0.021	0.026	0.028	0.06	0.05	0.059	0.057	0.050
iC_4H_{10}/%	0.001	0.002	0	0.002	0.002	0.005	0.004	0.005	0.004	0.004
nC_4H_{10}/%	0.001	0.002	0.001	0.002	0.002	0.005	0.005	0.006	0.005	0.005
iC_5H_{12}/%	0.000	0	0.000	0	0.000	0.002	0.002	0.002	0.001	0.002
nC_5H_{12}/%	0.000	0.002	0.000	0.000	0.000	0.001	0.001	0.001	0.001	0.001
C_6/%	0.002	0.002	0.001	0.001	0.002	0.003	0.003	0.003	0.003	0.003
C_7/%	0.007	0.008	0.010	0.005	0.011	0.000	0.000	0.000	0.000	0.000
C_8/%	0.001	0.001	0.000	0.000	0.000	0.000	0.000	0.000	0.000	0.000
H_2/%	0.000	0.000	0.084	0.253	1.206	0.021	0.034	0.032	0.031	0.030
N_2/%	0.784	0.598	4.103	0.927	0.796	0.758	0.910	0.796	0.938	0.922
CO_2/%	2.432	2.432	1.382	2.376	0.55	1.157	1.263	0.902	1.23	1.12
Relativedensity(T = 20℃)	0.5837	0.5836	0.5869	0.5834	0.5606	0.5732	0.5744	0.5708	0.5744	0.5730
Density(T = 20℃)/kg/m^3	0.7031	0.7030	0.7069	0.7027	0.6753	0.6904	0.6919	0.6874	0.6918	0.6902
Lowcalorificvalue(T = 20℃)/MJ/kg	32.5	32.6	31.7	32.431	32.9	33.013	32.902	33.076	32.909	32.942
Highcalorificvalue(T = 20℃)/MJ/kg	36.00	36.20	35.1	36	36.5	36.642	36.519	36.71	36.53	36.56
Total	100	100	100	100	100	100	100	100	100	100

Table 3 Composition of 30 groups of natural gas samples-b

Sample	11	12	13	14	15	16	17	18	19	20
CH_4/%	97.149	95.238	96.052	96.194	95.206	96.781	96.605	96.991	96.937	95.836
C_2H_6/%	0.691	0.748	0.582	0.671	1.91	0.685	0.791	0.791	0.743	0.442
C_3H_8/%	0.07	0.109	0.057	0.063	0.141	0.069	0.079	0.068	0.066	0.043
iC_4H_{10}/%	0.005	0.009	0.005	0.006	0.010	0.007	0.009	0.008	0.007	0.006
nC_4H_{10}/%	0.006	0.010	0.006	0.006	0.015	0.007	0.009	0.008	0.007	0.006
iC_5H_{12}/%	0.002	0.003	0.002	0.002	0.004	0.002	0.004	0.003	0.003	0.002
nC_5H_{12}/%	0.001	0.001	0.001	0.001	0.001	0.001	0.001	0.001	0.001	0.001
C_6/%	0.003	0.001	0.001	0.002	0.003	0.002	0.003	0.003	0.003	0.003
C_7/%	0.000	0.000	0.000	0.000	0.000	0.000	0.000	0.000	0.000	0.001
C_8/%	0.000	0.000	0.000	0.000	0.000	0.000	0.000	0.000	0.000	0.000
H_2/%	0.032	0.028	0.024	0.039	0.000	0.031	0.032	0.064	0.063	0.019
N_2/%	0.955	2.687	0.794	0.851	0.323	0.848	0.946	0.890	0.934	0.646
CO_2/%	1.084	0.939	2.273	2.162	2.384	1.563	1.514	1.168	1.23	2.99
Relativedensity(T = 20℃)	0.5734	0.5812	0.5856	0.5832	0.5905	0.5776	0.5783	0.5744	0.5749	0.5893
Density(T = 20℃)/kg/m^3	0.6907	0.7000	0.7053	0.7025	0.7112	0.6957	0.6966	0.6919	0.6925	0.7098
Lowcalorificvalue(T = 20℃)/MJ/kg	32.976	32.41	32.531	32.641	33.132	32.853	32.877	32.994	32.942	32.371
Highcalorificvalue(T = 20℃)/MJ/kg	36.60	35.97	36.108	36.229	36.758	36.463	36.489	36.62	36.56	35.92
Total	100	100	100	100	100	100	100	100	100	100

Table 4 Composition of 30 groups of natural gas samples-c

Sample	21	22	23	24	25	26	27	28	29	30
CH_4/%	96.4	96.019	96.097	95.883	97.631	95.127	95.511	95.493	95.487	95.370
C_2H_6/%	0.649	0.676	0.668	0.457	0.644	0.4	0.401	0.408	0.373	0.412
C_3H_8/%	0.061	0.105	0.099	0.039	0.059	0.029	0.031	0.031	0.027	0.031
iC_4H_{10}/%	0.005	0.010	0.013	0.003	0.006	0.007	0.005	0.006	0.000	0.007
nC_4H_{10}/%	0.006	0.006	0.006	0.000	0.006	0.000	0.000	0.000	0.000	0.000
iC_5H_{12}/%	0.002	0.002	0.002	0.000	0.000	0.000	0.000	0.000	0.000	0.000
nC_5H_{12}/%	0.001	0.001	0.001	0.000	0.000	0.000	0.000	0.000	0.000	0.000
C_6/%	0.002	0.000	0.000	0.000	0.000	0.000	0.000	0.000	0.000	0.000
C_7/%	0.000	0.000	0.000	0.000	0.000	0.000	0.000	0.000	0.000	0.000
C_8/%	0.000	0.000	0.000	0.000	0.000	0.000	0.000	0.000	0.000	0.000
H_2/%	0.029	0.000	0.000	0.000	0.000	0.000	0.000	0	0.000	0.000
N_2/%	0.699	0.711	0.734	0.658	1.570	0.507	0.522	0.522	0.533	0.540
CO_2/%	2.142	2.468	2.38	2.96	0.084	3.91	3.53	3.540	3.58	3.64
Relativedensity(T = 20℃)	0.5824	0.5862	0.5854	0.5888	0.5659	0.597	0.5934	0.5936	0.5937	0.5947
Density(T = 20℃)/kg/m^3	0.7014	0.7061	0.7051	0.7092	0.6816	0.7191	0.7127	0.7149	0.7151	0.7163
Lowcalorificvalue(T = 20℃)/MJ/kg	32.695	32.62	32.63	45.64	48.54	44.62	45.06	45.05	44.99	44.9
Highcalorificvalue(T = 20℃)/MJ/kg	36.289	36.20	36.22	50.66	53.88	49.53	50.02	50.00	49.94	49.85
Total	100	100	100	100	100	100	100	100	100	100

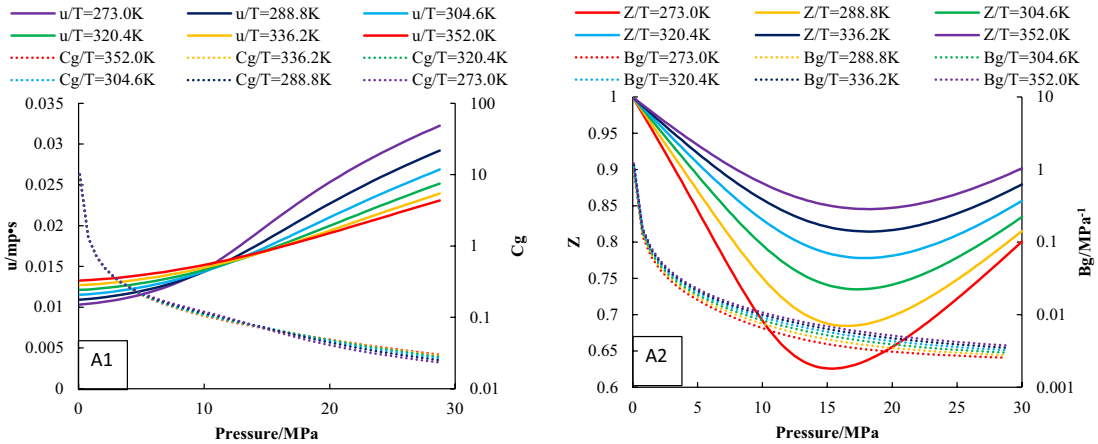

Fig. 11 Property curve of natural gas (A1: P–μ curve of natural gas and P–C_g curve of natural gas; A2: P–Z curve of natural gas and P–B_g curve of natural gas)

However, the viscosity and compressibility of natural gas vary with pressure (Fig. 12); therefore, Eq. (1) is not valid.

By deforming Eq. (1):

$$\frac{\partial\left(\overline{P}/\overline{Z}\right)}{\partial G_{\mathrm{P}}}=\frac{\partial\left(\overline{u_g}\overline{C_g}\right)}{\partial\left(u_{\mathrm{gwf}}C_{\mathrm{gwf}}\right)}\cdot\frac{\partial\left(P_{\mathrm{wf}}/Z_{\mathrm{wf}}\right)}{\partial G_{\mathrm{P}}} \tag{2}$$

$$\frac{\partial\left(\overline{u_{\mathrm{g}}}\overline{C_g}\right)}{\partial\left(u_{\mathrm{gwf}}C_{\mathrm{gwf}}\right)}\approx\frac{\left(u_gC_g\right)\big|_{\overline{P_{\mathrm{pss}}}}}{\left(u_gC_g\right)\big|_{P_{\mathrm{wf}}-pss}}\approx\frac{\left(u_gC_g\right)\big|_{p_{\mathrm{i}}}}{\left(u_gC_g\right)\big|_{P_{\mathrm{wf}}-pss}}=\lambda \tag{3}$$

The steps of the modified FMB are as follows (Fig. 13):

(1) According to the relationship between p and $\mu_g c_g$, $\left(u_gc_g\right)\big|_{pi}$ and $\left(u_gc_g\right)\big|_{p_{wf-pss}}$ can be gotten.

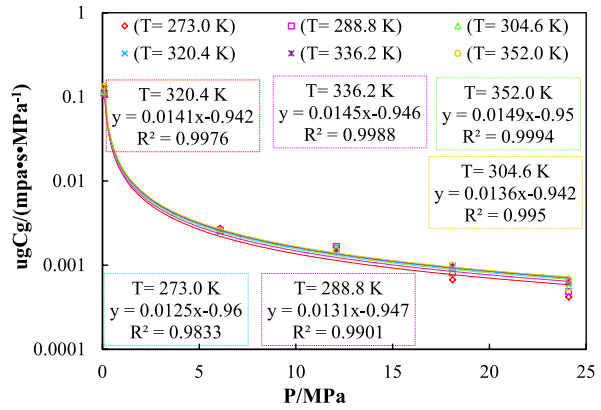

Fig. 12 P–u_gC_g curve of natural gas

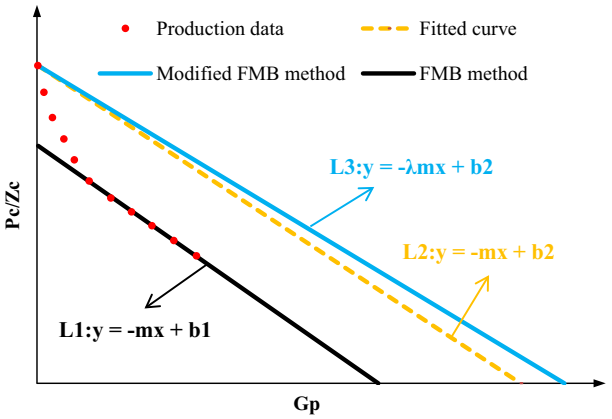

Fig. 13 Process of modified FMB method

(2) The *-m* can be got with the bottom hole pressure and cumulative production data (P_{wf}~Z_{wf}~G_p).
(3) Make a straight line over P_i/Z_i with the slope of $-\lambda m$, and the intercept is the reserves determined by the modified FMB (modified G_i).
(4) Similarly, the wellhead casing pressure P_c is used to replace the bottom hole pressure P_{wf}.

Result

According to reservoir characteristics and pore structure, the gas wells in the study area can be divided into three types: I, II and III. The production law of the three types of gas wells is analyzed. At the same time, the controlled reserves are calculated by using the established modified FMB.

Type-I

The initial production of Type-I wells in Yan'an gas field is high, and the pressure drops slowly, so it has a good productivity under the condition of low pressure (Fig. 14). The OFR of Type-I well is the largest, with average of $30.57\times10^4m^3/d$. The average monthly production is $95\times10^4m^3/m$ and the decline pattern is at a low level with 17.9% at the initial stage. The casing pressure and the production decrease slowly in the second stage. The production was kept at a middle level and casing pressure is about 8.6 MPa in the third stage.

The results show that the dynamic reserve of Type-I well are $1.398\times10^8m^3$ with FMB and $1.906\times10^8m^3$ with modified FMB (Fig. 15).

Type-II

The OFR of Type-II is middle. The average production is $79\times10^4m^3/d$ and the decline rate is 37.32% from the production curve (Fig. 14). After the production is reduced by $1\times10^4m^3/d$, the casing pressure decreases from 14.41 to 8.36 MPa. Up to June 2017, the cumulative gas production is $2273.123\times10^4m^3$.

The results show that the dynamic reserve of Type-II is $0.807\times10^8m^3$ with FMB and $1.233\times10^8m^3$ with modified FMB (Fig. 15).

Type-III

The OFR of Type-III well is the lowest, with average $6.2\times10^4m^3/d$ from the production curve (Fig. 14). It has been in production since August 2015 and the average monthly production is $27\times10^4m^3/m$ at the initial stage. The casing pressure decreases rapidly and the monthly production remained unchanged in the second stage. Up to now, the cumulative production of Type-III is $352.896\times10^4m^3$.

The results show that the dynamic reserve of Type-III well is $0.787\times10^8m^3$ with FMB and $11{,}186.93\times10^8m^3$ with modified FMB (Fig. 15).

Discussion

Compared with the FMB, the MB uses the average formation pressure measured after shut-in for a long time, so it is more reliable.

Method verification

In order to verify the accuracy of the calculation of the modified FMB, the diagram between the cumulative production and the *P/Z* is drawn with the formation pressure at different stages, as shown in Table.5, Fig. 16.

The dynamic reserves calculated of three wells by MB can be obtained. ①The reserve of Type-I is $1.87\times10^8m^3$. The error of FMB is 25.33% and the modified FMB is 1.79%

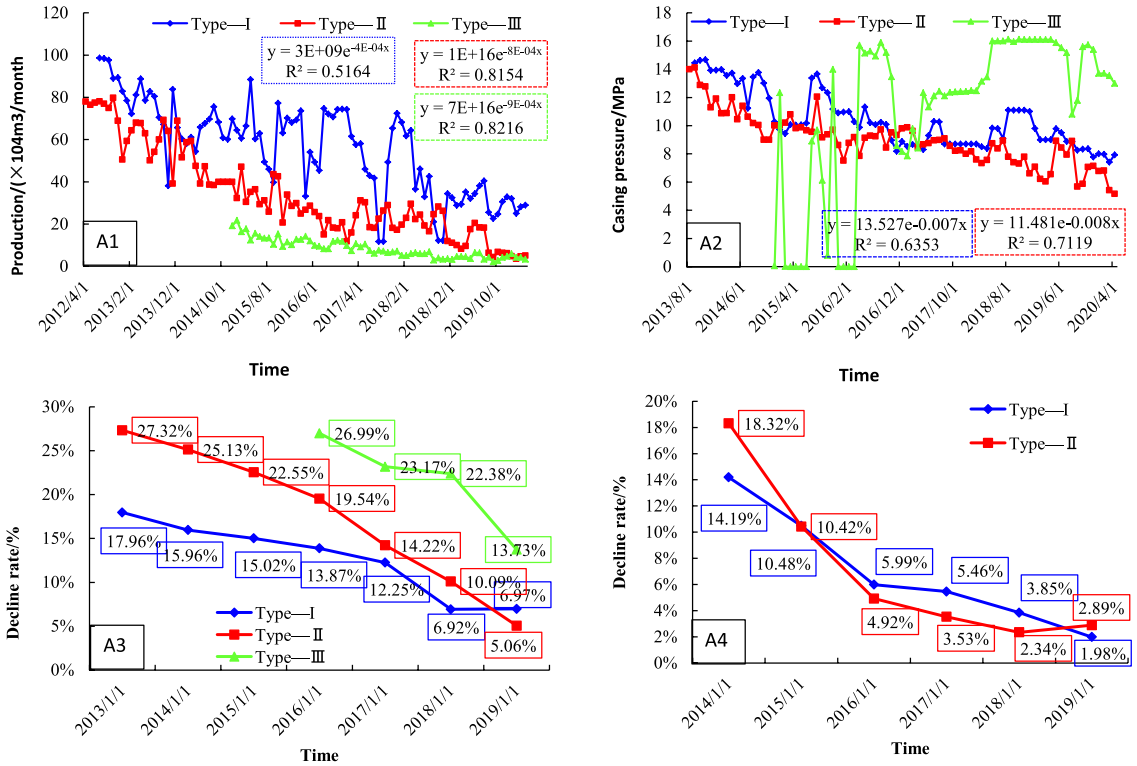

Fig. 14 Decline pattern of wells (A1: production; A2: surface casing pressure; A3: production decline rate; A4: decline rate of surface casing pressure)

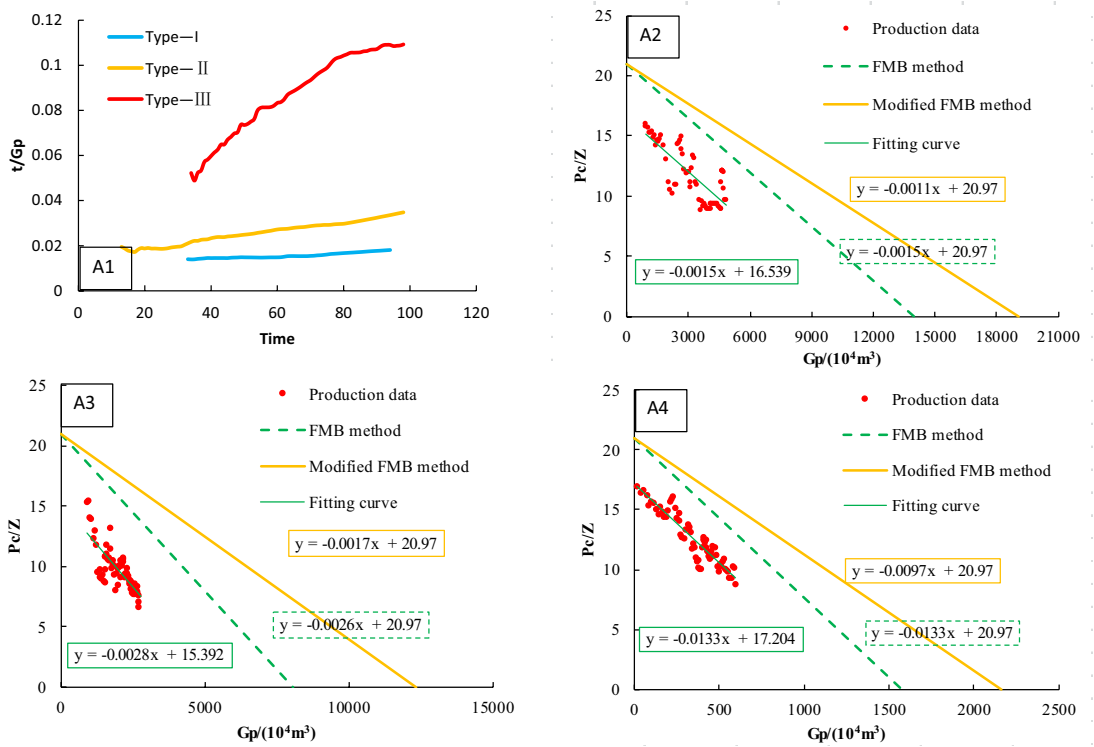

Fig. 15 Calculation results of dynamic reserves by modified FMB method (A1: decline characteristic; A2: Type-I wells; A3: Type-II wells; A4: Type-III wells)

Table 5 Measured pressure of three wells

Time	Type-I			Type-II			Type-III		
	Gp/10^4m^3	P/MPa	P/Z	Gp/10^4m^3	P/MPa	P/Z	Gp/10^4m^3	P/MPa	P/Z
201,41212/2014	2022.636	18.567	20.313	1521.516	19.727	21.608	19.142	18.959	20.784
201,50606/2015	2542.779	18.018	19.735	1672.240	19.091	20.862	117.142	18.108	19.834
201,51212/2015	2890.334	17.589	19.228	1859.788	18.893	20.710	190.513	17.462	19.122
201,60606/2016	3293.128	17.152	18.646	2024.006	18.273	20.036	253.299	16.932	18.513
201,61212/2016	3659.213	16.186	17.661	2141.368	17.988	19.674	306.868	16.520	17.993
201,70606/2017	4041.439	15.915	17.292	2273.123	17.069	18.619	352.896	16.215	17.542

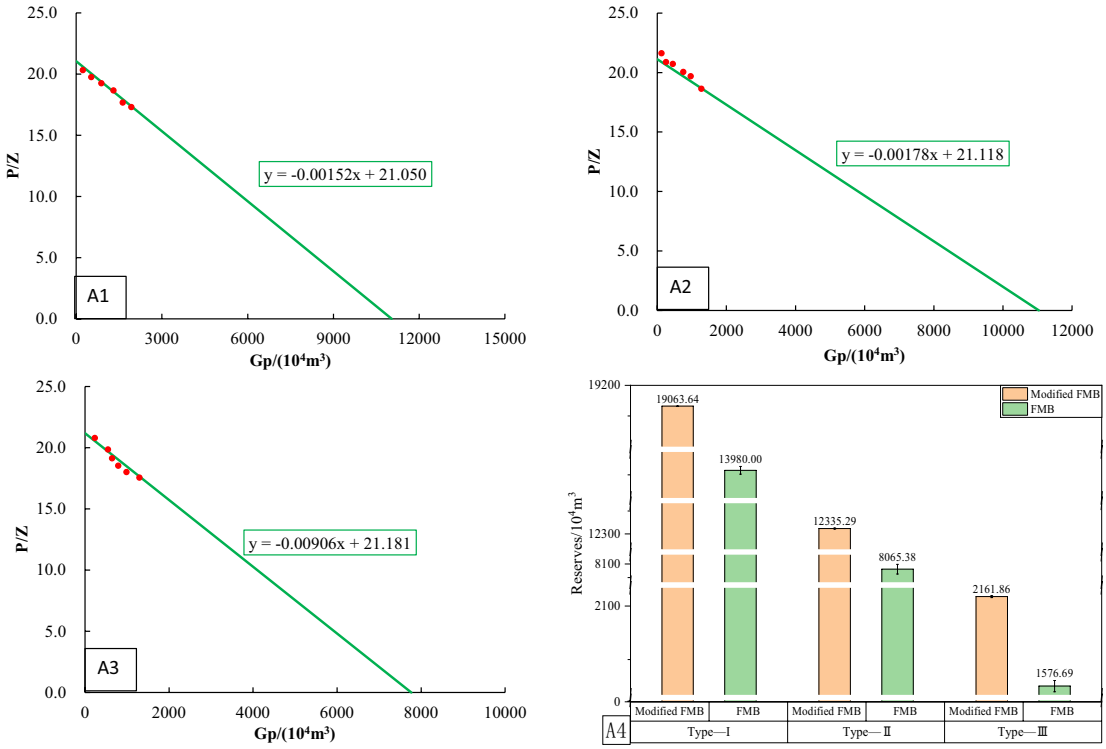

Fig. 16 Calculation of dynamic reserves by MB

Table 6 Calculation results of FMB method and modified FMB method

Well	MB/10^4m^3	FMB/10^4m^3	Error/%	Modified FMB/10^4m^3	Error/%
Type-I	18,723.21	13,980.00	25.33	19,063.64	1.79
Type-II	11,864.04	8065.38	32.02	12,335.29	3.82
Type-III	2017.24	1576.69	36.73	2161.86	6.69
Average	10,868.17	7874.03	31.36	11,186.93	4.10

(Table.6, Fig. 16).②The reserve of Type-II is $1.18\times10^8m^3$. The error of FMB and the error of modified FMB are 32.02% and 3.82%.③The reserve of Type-III is $0.20\times10^8m^3$, with the error of FMB of 36.73% and the error of modified FMB of 6.69%.

Through the above calculation, compared with the MB, the result of the FMB is generally small, with an average error of 31.36%; the error of the modified FMB is small, with an average of 4.10%. Therefore, the method established in this paper can provide scientific guidance for the determination of single-well dynamic reserves in tight sandstone reservoirs.

Table 7 Calculation results of three dynamic reserve methods

WELL	MB	FMB		Modified FMB	
	Reserves /10^4m^3	Reserves /10^4m^3	Error /%	Reserves /10^4m^3	Error /%
YA-1	1.233	0.865	29.90	1.232	0.10
YA-2	0.929	0.648	30.27	0.932	0.27
YA-3	0.929	0.645	30.58	0.934	0.58
YA-4	0.885	0.644	27.31	0.862	2.69
YA-5	0.884	0.577	34.66	0.925	4.66
YA-6	0.877	0.640	27.08	0.852	2.92
YA-7	0.872	0.651	25.34	0.831	4.66
YA-8	0.864	0.607	29.76	0.862	0.24
YA-9	0.859	0.619	27.98	0.842	2.02
YA-10	0.859	0.601	30.04	0.859	0.04
YA-11	0.858	0.624	27.27	0.835	2.73
YA-12	0.841	0.604	28.16	0.825	1.84
YA-13	0.798	0.575	27.97	0.782	2.03
YA-14	0.787	0.571	27.43	0.767	2.57
YA-15	0.773	0.563	27.10	0.750	2.90
YA-16	0.767	0.550	28.26	0.753	1.74
YA-17	0.765	0.553	27.70	0.748	2.30
YA-18	0.758	0.554	26.85	0.734	3.15
YA-19	0.756	0.542	28.32	0.744	1.68
YA-20	0.749	0.538	28.14	0.735	1.86
YA-21	0.732	0.549	25.03	0.696	4.97
YA-22	0.688	0.495	28.08	0.674	1.92
YA-23	0.687	0.502	26.91	0.666	3.09
YA-24	0.681	0.505	25.76	0.652	4.24
YA-25	0.676	0.488	27.79	0.661	2.21
YA-26	0.673	0.470	30.16	0.674	0.16
YA-27	0.663	0.486	26.65	0.641	3.35
YA-28	0.663	0.496	25.19	0.631	4.81
YA-29	0.658	0.463	29.61	0.656	0.39
YA-30	0.641	0.436	32.01	0.654	2.01
Min	0.129	0.088	25.03	0.133	0.04
Max	1.233	0.865	34.66	1.232	4.97
Average	0.523	0.372	28.87	0.516	2.45

Application

Three dynamic reserve methods are used to calculate 88 wells, and the results are shown in Table.7 (More calculation are in the Supplementary online). The average reserves calculated by the MB and the FMB are $0.523\times10^8m^3$, $0.372\times10^8m^3$, respectively, and the average error of FMB is 28.87%. The result of modified FMB is $0.516\times10^8m^3$, with minimum error of 0.04%, the maximum error of 4.97% and the average error of 2.45%.

Conclusion

(1) Controlled by sedimentary, the pore structure in the study area can be divided into three types based on the morphology of the capillary pressure and the analysis of the reservoir characteristics: Type-I, Type-II and Type-III.

(2) The viscosity of natural gas increases rapidly with pressure through theoretical calculation and numerical simulation. The compressibility decreases when pressure is less than 15 MPa and then increases when pressure is great than 15 MPa, and increases with temperature monotonically. Then, the results calculated by the FMB are smaller when the effect of pressure on viscosity and compressibility is not considered.

(3) Considering the viscosity and compressibility, the modified FMB and the calculation steps are given. The results of three typical wells show that compared with the results of the MB, the average error of the FMB is 31.36%, and the average error of the modified FMB is 4.10%.

(4) The calculation of 88 wells shows that the error of FMB is 28.87% and the error of modified FMB is only 2.45%. Therefore, the proposed method in the paper can quickly and accurately calculate the dynamic reserves of single well in tight reservoir.

Supplementary Information The online version contains supplementary material available at https://doi.org/10.1007/s13202-022-01584-0.

Funding Funding was provided by National Major Science and Technology Projects of China (Grant Number 2017ZX05008-004-004-001).

Declarations

Conflict of interest On behalf of all the co-authors, the corresponding author states that there is no conflict of interest.

References

Andersen JP, Hyman B (2001) Energy and material flow models for the US steel industry. Energy 26(2):137–159

Clarkson CR (2013) Production data analysis of unconventional gas wells: review of theory and best practices. Int J Coal Geol 109:101–146

Feng Z, Liu D, Huang S, Gong D, Peng W (2016) Geochemical characteristics and genesis of natural gas in the Yan'an gas field, Ordos Basin, China. Org Geochem 102:67–76

Guo S, Lyu X, Zhang Y (2018) Relationship between tight sandstone reservoir formation and hydrocarbon charging: a case study of a Jurassic reservoir in the eastern Kuqa Depression, Tarim Basin, NW China. J Nat Gas Sci Eng 52:304–316

Han G et al (2019) Determination of pore compressibility and geological reserves using a new form of the flowing material balance method. J Petrol Sci Eng 172:1025–1033

He J et al (2021) Experimental study on the two-phase seepage law of tight sandstone reservoirs in ordos Basin. J Energy Eng 147(6):04021056

Hirst JPP, Davis N, Palmer AF, Achache D, Riddiford FA (2001) The "tight gas" challenge: appraisal results from the Devonian of Algeria. Pet Geosci 7(1):13–21

Hu A et al (2008) Geochemical characteristics and origin of gases from the upper, lower paleozoic and the Mesozoic reservoirs in the Ordos Basin, China. Sci China Ser D-Earth Sci 51:183–194

Hu G, Li J, Shan X, Han Z (2010) The origin of natural gas and the hydrocarbon charging history of the Yulin gas field in the Ordos Basin. China Int J Coal Geol 81(4):381–391

Kanianska R, Gustafikova T, Kizekova M, Kovanda J (2011) Use of material flow accounting for assessment of energy savings: a case of biomass in Slovakia and the Czech Republic. Energy Policy 39(5):2824–2832

Li B, He D, Ning B, Ji G, Li X (2015) A new method of evaluating well controlled reserves of horizontal wells in tight gas sandstone reservoirs. Geol Sci Tech Inf 34(2):174–180

Long S et al (2011) Formation mechanism of the Changxing formation gas reservoir in the Yuanba gas field, Sichuan Basin. China Acta Geol Sin-Engl Ed 85(1):233–242

Luo R et al (2019) Evaluation of dynamic reserves in ultra-deep naturally fractured tight sandstone gas reservoirs, international petroleum technology conference, pp. D021S041R006.

Lyu X, Zhu G, Liu Z (2020) Well-controlled dynamic hydrocarbon reserves calculation of fracture-cavity karst carbonate reservoirs based on production data analysis. J Pet Explor Prod Technol 10(6):2401–2410

Mattar L, Anderson D, Stotts G (2006) Dynamic material balance - oil- or gas-in-place without shut-ins. J Can Pet Technol 45(11):7–10

Muther T et al (2022a) Unconventional hydrocarbon resources: geological statistics, petrophysical characterization, and field development strategies. J Pet Explor Prod Technol 12(6):1463–1488

Muther T, Syed FI, Dahaghi AK, Negahban S (2022b) Socio-inspired multi-cohort intelligence and teaching-learning-based optimization for hydraulic fracturing parameters design in tight formations. J Energy Resour Technol-Trans Asme 144(7):073201

Nie X, Chen J, Yuan S (2018) Experimental study on stress sensitivity considering time effect for tight gas reservoirs. Mechanika 24(6):784–789

Ning N et al (2009) The unconventional natural gas resources and exploitation technologies in China. Nat Gas Ind 29(9):9–12

Ruilan L, Qun L, Yongxin H, Jinde F and Chunhong M, (2010) A new method for forecasting dynamic reserve of fractured gas well in low-permeability and tight gas reservoir, international oil and gas conference and exhibition in China, pp. SPE-130755-MS.

Schmoker JW (2002) Resource-assessment perspectives for unconventional gas systems. AAPG Bull 86(11):1993–1999

Shults OV (2020) Method for calculating material balance of complex process flowcharts. J Math Chem 58(6):1281–1290

Sun H et al (2020) A material balance based practical analysis method to improve the dynamic reserve evaluation reliability of ultra-deep gas reservoirs with ultra-high pressure. Nat Gas Ind 40(7):49–56

Wang Y et al (2013) Comparison of ordos and foreign similar basins and prediction for Mesozoic oil reserves in Ordos Basin. Geoscience 27(5):1244–1250

Wei Y, Ran Q, Li R, Yuan J, Dong J (2016) Determination of dynamic reserves of fractured horizontal wells in tight oil reservoirs by multi-region material balance method. Pet Explor Dev 43(3):490–498

Zhang J-C, Tang X, Jiang S-L, Bian R-K (2008) Natural gas accumulating and distribution spectra in clastic basins. Nat Gas Ind 28(12):11–17

Zhenhua C. and Xinwei L, (2013) A new calculation method for single well controlled dynamic reserves of tight gas, international petroleum technology conference, pp. IPTC-17184-MS.

Zou C et al (2012) Tight gas sandstone reservoirs in China: characteristics and recognition criteria. J Petrol Sci Eng 88–89:82–91